DOI: 10.61782/fa.2025.0428

HIERARCHICAL LABYRINTHINE METAMATERIALS FOR LOW FREQUENCY NOISE ABSORPTION APPLICATIONS

Pérez Compte, Eloi[1*] **Nistri, Fabio**[1] **Zambila, Liviu**[2]
Bergamini, Andrea[2] **Gliozzi, Antonio**[1] **Shtrepi, Louena**[3] **Bosia, Federico**[1]
[1] Department of Applied Science and Technology, Politecnico di Torino, Turin, Italy
[2] Swiss Federal Laboratories for Materials Science and Technology, EMPA, Dübendorf, Switzerland
[3] Department of Energy, Politecnico di Torino, Turin, Italy

ABSTRACT

We present a proof-of-concept experiment demonstrating the efficient noise absorption of a 3-D printed metamaterial panel. The panel consists of an arrangement of unit cells designed using a fractal-inspired geometry from which a relation between the level of iteration and resonance frequency is derived. An analytical model and numerical simulations are used to study the absorption characteristics of the single labyrinthine units, and optimization methods derived from the causality principle are employed to find the optimal arrangement of unit cells to enhance the absorption performance in the low frequency range (~ 300 Hz). The performance of the panel is experimentally validated in fully anechoic room, using an impulsive sound source separation technique. Results show close to ideal values of absorption at the desired frequency of operation in a subwavelength regime with a wavelength to thickness ratio of 27.5 for a panel 50 mm thick. This work suggests a design procedure for noise-mitigation panel solutions and provides experimental evidence of the versatility and effectiveness of hierarchical coiled-up metamaterials in providing tunable low-frequency sound attenuation with relatively thin structures.

Keywords: *Hierarchical, Labyrinth, Broadband, Low frequency, Panel*

*__*Corresponding author*__: *eloi.perezcompte@polito.it.*

1. INTRODUCTION

Acoustic metamaterials (AMs) have gained growing attention because of their exotic properties, which are not found in naturally occurring materials. AMs design parameters offer the possibility of developing a new generation of acoustic absorbers and diffusers tailored for a desired frequency spectrum and with sub-wavelength sizes [1] and low-frequency absorption [2]. AMs are thus able to achieve high performance in terms of noise reduction, and simultaneously reduce the size and weight of structures [3], going beyond the limitations of conventional technologies based on porous absorbers or resonant structures coupled with air [4]. AMs are employed as acoustic sound absorbers with which perfect absorption can be obtained at their resonance frequency, by design. This occurs for a critical coupling condition: thermo-viscous losses are exactly balanced by energy leakage [5]. Thus, to extend the effect on a broader frequency range, the design concept of 'rainbow trapping' is exploited combining acoustic resonators with variable parameters, and hence working frequencies [6] or systems with asymmetric porous absorbers [7].

With the aim of reducing the volume occupied by these AM absorbers, 'labyrinthine' or 'coiled' structures were brought up [8, 9]. These are based on exploiting acoustic wave propagation in curved channels of sub-wavelength cross-section, giving rise to an extremely high effective refractive index (and thus to a decrease of the effective wave speed). Fractal inspired design with the aim of tuning the resonance frequency range, reducing the volume encumbrance have been investigated and experimentally characterized [9–11]. Thus, labyrinthine and space-filling AMs have provided a very convenient and efficient way to achieve sound control in large frequency ranges, especially in the subwavelength regime, by tuning geometrical design parameters (e.g. channel tortuosity or elongation and cavity size). This kind of adaptability could largely benefit noise absorption applications at small to medium scale, in comparison with thick conventional acoustic absorbing materials. At present, few studies in the literature have presented detailed acoustic characterization studies on large structures such as metamaterial-based panels, and none on labyrinthine ones, to the best of our knowledge. Further, the need emerges to investigate labyrinthine AM performance on structures that are closer to potential operating conditions, i.e. in free field.

2. METHODS

2.1 Unit cell design

The design of the Unit Cell (UC) shown in fig. 1a corresponds to the second iteration of the Wunderlich curve. This system can be simplified to two connected waveguides of different cross section for the orifice and the coiled-up channel. While the orifice acts as a pore, the channel works as a quarter wavelength resonator and its resonance frequency can be computed as $f_0 = 4c/L_{eff}$, where $c = 343$ m/s is the speed of sound in air, and L_{eff} is the effective length of the tube. With the same design principle of [9], a 3D UC is designed (fig. 1b). Due to the narrower size of both the orifice and the channel compared to the wavelength, thermoviscous losses have to be taken into account. These physical dissipation mechanisms effectively absorb sound energy, leading to perfect absorption when they are balanced by the acoustic energy leakage by radiation from the UC: the matching of the two correponds to the critical coupling condition [5]. Thus combining the Stinson's and Johnson-Champoux-Allard models for the coiled-up channel and the orifice, respectively, we can compute the impedance Z_s at the aperture of the UC, from we which we can compute the absorption spectrum:

$$\alpha = 1 - \mid \frac{Z_s - Z_0}{Z_s + Z_0} \mid^2, \tag{1}$$

where Z_0 is the characteristic impedance of air. A parametric study of the analytical model is carried out (fig.1c) to study the dependence of maximum sound absorption on the edge size a, ranging from $20-60$ mm, and the aperture cross section t from approximately $10-50$ mm. From this four-parameter map a UC of size $a = 20$ mm and $t = 15$ mm is selected and numerically characterized, showing good agreement with the analytical prediction (fig.1d).

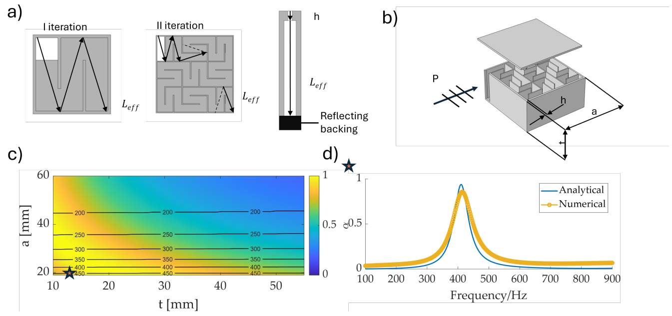

Figure 1. (a) Exploded view of the UC and its lid. (b, left) Top view of the coiled up structure and effective length path with (right) schematic of its equivalent model. (c) Four parameter map of absorption peak as a function of the UC cell size a and thickness t

2.2 Panel design and fabrication

Establishing the target frequency for sound absorption around 300 Hz, we use analytical data to design the sound absorption panel. This can be achieved by exploiting various UCs of different effective length, corresponding to different resonance frequencies arranged in a exponential progression, to maximize the absorption spectrum over the target frequency range [3]. An AM panel is thus designed, consisting of differently sized UCs. The internal wall thickness of each UC is 2 mm and their height of 20 mm. 6 UCs have been selected with edge size a ranging from 38.5 to 40.2 mm and assembled together in a row, as shown in fig. 2a. The complete panel consists of the combination of 87 macro-cells arranged in the plane (2b), to total size of $775 \times 640 \times 43$ mm. The UCs are selected so as to provide different absorption peaks, whose superposition provides a wider working frequency spectrum in the chosen target frequency range. The overall impedance of the panel can be calculated as the combination in parallel of the impedances of the single UCs. The polyamide panel is then manufactured through selective laser sintering (SLS), a technique where each level is sintered by a laser beam, directed by a scanning system. The process is repeated, and the prototype is built layer by layer.

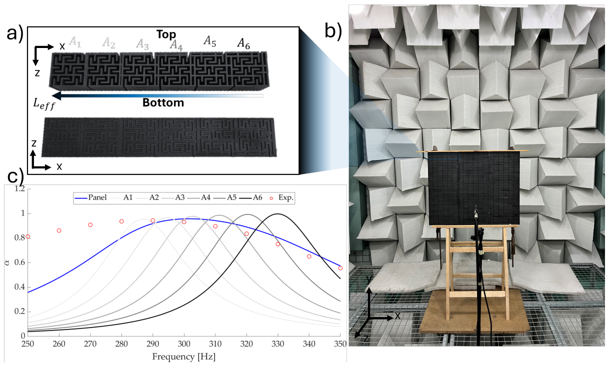

Figure 2. (a) Top and bottom view of the macrocell featured by 6 UCs of different edge size, i.e. L_{eff}. (b) Experimental setup in anechoic chamber. (c) Absorption spectra analytical prediction compared with the experimental result.

2.3 Experimental determination of sound reflection characteristics

In order to measure the performance of the hierarchical panel in a free field condition, all measurements were performed in a fully anechoic room. The setup consisted in placing the panel and the loudspeaker in front of each other and fixing their respective position. Then, between the panel and the loudspeaker, a grid of microphones should be placed, in order to measure the scattered field from different positions and take account of the boundary effects such as the diffraction by the edge of the panel. In our case, repeated measurements with a single microphone were made, placing it at each respective point of the grid, in order to have an equivalent system. The position of the panel and the microphone in the anechoic room can be seen in figure 2b. The measurement grid points were chosen along the horizontal and vertical middle line of the panel. The input signal sent to the loudspeaker consisted of three consecutive exponential sweeps, each generated according the the following function:

$$x(t) = \sin\left[2\pi f_1 \exp\left(\frac{N f_s \ln(f_2/f_1)}{T} t\right)\right] / f_s \,, \quad (2)$$

where f_s is the sampling rate, f_1 and f_2 are the start and end frequencies of the sweep, N is the length of the signal and T is the sweep duration.

2.4 Signal processing

Once the output signal $y(t)$ is measured, some processing must be done to get the reflection index of the panel.

First, for each microphone placement, three consecutive sweeps were sent. By performing a cross-correlation with the input signal, we could synchronize and cut the sweeps in order to perform an average, removing a significant amount of noise. The signal was then deconvoluted to obtain the impulse response $h(t)$ by means of a convolution with the inverse sweep defined as:

$$x_{\text{inv}} = x(-t) \exp\left[-\frac{t}{T} \ln\left(\frac{f_2}{f_1}\right)\right]. \quad (3)$$

For obtaining the reflected field without the contribution of the incident field, we used the signal subtraction technique. It consists in subtracting the free field impulse response to which an appropriate amplitude correction has been applied, to the scattered field impulse response.

In order to avoid unwanted reflections, an Adrienne window composed of a leading edge having a left Blackman-Harris shape, followed by a flat portion and closing with a trailing edge having a right Blackman-Harris shape was applied to the impulse response. With that, we were able to compute the Fast Fourier Transform (FFT) of both the incident and the reflected fields in order to get the Frequency Response Functions (FRF) $H_{i,k}(f)$ and $H_{r,k}(f)$ for each measurement point k of the incident and reflected fields respectively.

The reflection index is calculated as follows:

$$R(f) = \frac{1}{n} \sum_{k=1}^{n} \left[\frac{|H_{r,k}(f)|^2}{|H_{i,k}(f)|^2} C_{\text{geo},k}\right] \quad (4)$$

where the correction factor for geometrical divergence $C_{\text{geo},k}$ is:

$$C_{\text{geo},k} = \left(\frac{d_{r,k}}{d_{i,k}}\right)^2, \quad (5)$$

and $d_{i,k}$ is the distance from the front panel of the loudspeaker to the k-th measurement point and $d_{r,k}$ is the distance from the front panel of the loudspeaker to the source and microphone reference plane and back to the k-th measurement point following specular reflection.

Finally, he absorption coefficient of the panel is simply:

$$\alpha = 1 - |R|^2. \quad (6)$$

3. RESULTS

The absorption coefficient has been calculated analytically and measured experimentally in the range of frequencies where the largest absorption was expected. The length of the unit cells were tuned for the absorption peaks of the quarter-wavelength resonators to cover a the interval of 280 to 330 Hz as shown in figure 2c. Experimentally, the panel has a wide peak at the same interval with perfect absorption close to 290 Hz, shown by the red dots in figure 2c.

Indeed, the panel has a thickness of the order of 50 mm, and it can absorb acoustic waves of wavelength $\lambda = c/f$ of the order of one meter. With a wavelength to thickness ratio of ≈ 27.5 at the frequency for perfect absorption, the resonator shows sub-wavelength absorption properties, covering a range of about 50 Hz around the perfect absorption frequency before the absorption decays.

4. CONCLUSIONS

The present work shows the effectiveness of the designed panel in terms of broadband, low frequency, subwavelength absorption. The conception based in labyrinthine quarter-wavelength resonators optimizes their length to a limited surface area, allowing for low-frequency absorption capabilities in a limited space. The arranged design broadens the absorption spectrum while maintaining the width of the panel. Analytically, the design features of the panel were determined and tuned to achieve perfect absorption in the wanted frequency range. A polyamide panel was built, and, using a microphone measurement grid in an anechoic room and proper signal processing, we observed how the panel exhibits perfect absorption close to the analytical target frequency range, with a high wavelength to thickness ratio of about 27.5 confirming the subwavelength quality of the design.

5. REFERENCES

[1] X. Zhang, Z. Qu, and H. Wang, "Engineering acoustic metamaterials for sound absorption: from uniform to gradient structures," *Iscience*, vol. 23, no. 5, 2020.

[2] S. Kumar and H. P. Lee, "The present and future role of acoustic metamaterials for architectural and urban noise mitigations," in *Acoustics*, vol. 1, pp. 590–607, MDPI, 2019.

[3] J. Li, X. Wen, and P. Sheng, "Acoustic metamaterials," *Journal of Applied Physics*, vol. 129, no. 17, 2021.

[4] F. Langfeldt and W. Gleine, "Improved sound transmission loss of glass wool with acoustic metamaterials," *Proc 26th ICSV*, pp. 7–11, 2019.

[5] V. Romero-García, G. Theocharis, O. Richoux, and V. Pagneux, "Use of complex frequency plane to design broadband and sub-wavelength absorbers," *The Journal of the Acoustical Society of America*, vol. 139, no. 6, pp. 3395–3403, 2016.

[6] N. Jiménez, V. Romero-García, V. Pagneux, and J.-P. Groby, "Rainbow-trapping absorbers: Broadband, perfect and asymmetric sound absorption by subwavelength panels for transmission problems," *Scientific reports*, vol. 7, no. 1, p. 13595, 2017.

[7] J. Boulvert, T. Humbert, V. Romero-García, G. Gabard, E. R. Fotsing, A. Ross, J. Mardjono, and J.-P. Groby, "Perfect, broadband, and subwavelength absorption with asymmetric absorbers: Realization for duct acoustics with 3d printed porous resonators," *Journal of Sound and Vibration*, vol. 523, p. 116687, 2022.

[8] Z. Liang and J. Li, "Extreme acoustic metamaterial by coiling up space," *Physical review letters*, vol. 108, no. 11, p. 114301, 2012.

[9] F. Nistri, V. Kamrul, L. Bettini, E. Musso, D. Piciucco, M. Zemello, A. Gliozzi, A. Krushynska, N. Pugno, L. Sangiuliano, *et al.*, "Efficient broadband sound absorption exploiting rainbow labyrinthine metamaterials," *Journal of Physics D: Applied Physics*, vol. 57, no. 24, p. 245111, 2024.

[10] Y. Liu, W. Xu, M. Chen, T. Yang, K. Wang, X. Huang, H. Jiang, and Y. Wang, "Three-dimensional fractal structure with double negative and density-near-zero properties on a subwavelength scale," *Materials & Design*, vol. 188, p. 108470, 2020.

[11] A. O. Krushynska, F. Bosia, and N. M. Pugno, "Labyrinthine acoustic metamaterials with space-coiling channels for low-frequency sound control," *Acta Acustica United with Acustica*, vol. 104, no. 2, pp. 200–210, 2018.